A DETAILED DYNAMIC MODEL OF MULTI-STORY DOUBLE SKIN FACADES WITH INTEGRATED PHOTOVOLTAIC PANELS

Z. Ioannidis[1], A. Buonomano[2], A.K. Athienitis[1] , T. Stathopoulos[1]

[1] Centre for Zero Energy Building Studies, Department for Building, Civil and Environmental Engineering, Concordia University, 1455 de Maisonneuve Blvd. W., Montreal, Que., Canada, H3G 1M8

[2]DII, University of Naples Federico II, P.le Tecchio, 80, 80125 Naples, Italy

ABSTRACT

A numerical model is developed for a multi-story Double Skin Façade integrating Photovoltaics (DSF-P). The model has the ability to predict the thermal and electrical performance of the DSF-P system. The air flow inside the cavity may be assisted by a fan to cool down the photovoltaics while providing natural or hybrid ventilation to adjacent zones. Automated roller shades are implemented in the model and along with the shade that photovoltaics on the exterior skin provide, can control solar heat gains and daylight levels in the indoor space. A set of simulations was carried out for January and August in Montreal, for different air velocities inside the cavity, different roller blind positions and different number of floors. The simulations show that a DSF-P system integrating photovoltaics can supply approximately 0.20kWh/m^2/day of solar electricity to the adjacent office space covering the daily heating and cooling demand of the office.

Keywords: Double Skin Façade, BIPV, BIPV/T, Photovoltaics, multi-story, energy consumption.

INTRODUCTION

Double skin facades (DSF) are considered to be appropriate for buildings that are subject to great external noise and wind loads (Oesterle, 2001). Although the possibility of using solar radiation to satisfy all the energy needs of a building has led to the design and research of net-zero energy buildings (NZEB) (Athienitis & O'Brien, 2015). In this direction, DSF have a significant role and they are increasingly employed in high-rise buildings. DSF consist of an external and an internal skin separated by a cavity (Figure 1). This cavity is a buffer zone and it is created between the exterior skin and the insulated interior skin, which can be the façade of a newly built or renovated buildings. This cavity can also be naturally or hybrid ventilated and inside it, fixed or controllable shading devices can be installed. In this way, DSF can create a microclimate around the building adding climate resilience to it and letting it adapt to ambient temperature fluctuations. Temperature differences inside the cavity can be controlled in order to recover heat or coldness from it while the exterior skin can be a convenient base to integrate photovoltaics.

DSF, if well designed, can contribute to the reduction of the energy consumption of buildings by behaving as a buffer zone that can interact with the adjacent zones and the environment. Also DSF have significant potential for daylight control and energy savings through the use of louvers or blinds (Gratia & De Herde, 2007b; Manz, 2004; Saelens, Roels, & Hens, 2008), while a lot of work had been done studying these shading devices (e.g. position, blinds, roller thermal mass) (Quesada, Rousse, Dutil, Badache, & Hallé, 2012). In addition, DSF can improve acoustic comfort, protect the building from wind or rain penetration while it reduces the heating or cooling loads of the building (Gratia & De Herde, 2007a; Quesada et al., 2012; Shameri, Alghoul, Sopian, Zain, & Elayeb, 2011). In particular, to avoid rain penetration, one type of DSF, also named rainscreen wall, applies pressure equalization for which airflow and pressures inside the cavity are important (Kala, Stathopoulos, & Suresh Kumar, 2008). DSF also provide the opportunity to use operable windows and at the same time extend the usable indoor space area near the window. Furthermore, DSF can be an extremely suitable source for natural or hybrid ventilation for the building (Gratia & De Herde, 2007a).

The integration of photovoltaics on the exterior skin along with the implementation of controlled shading devices in the middle of the cavity of a DSF, give the opportunity to design an energy positive DSF façade. This can be achieved by combining three different features of the DSF:

- Electricity generation from the integrated opaque or semi-transparent photovoltaics.

- Solar heat gains and daylight control through the use of shading devices located between the exterior and interior skin of a DSF.
- Extraction of heat from the photovoltaics and the shading device which is recovered by the air flowing inside the cavity.

This technology has been widely reviewed in the past, concluding that the main research was focused on the ventilation of the DSF, whereas there is not extended research on daylighting (Shameri et al., 2011). In a recent study it is concluded that it is very difficult to achieve natural ventilation all year round and that a hybrid system should be developed (Barbosa & Ip, 2014). Since there was no standard way on reporting results among the researchers, De Gracia et al (De Gracia, Castell, Navarro, Oró, & Cabeza, 2013) suggested that further research is required to compare all models with the same experimental test, although many studies have focused only on the DSF cavity and not at its adjacent zones (Barbosa & Ip, 2014).

In addition to this topic, the available literature shows very few papers focused on the description of the behaviour of integrated photovoltaics on double skin façades. As an example, the heat transfer phenomena in an airflow window with BIPV/T were extensively studied (Liao et al., 2007), while the optimization of the performance of DSF with integrated opaque photovoltaics (Charron & Athienitis, 2006) and semi-transparent photovoltaics, (Gaillard, Giroux-Julien, Ménézo, & Pabiou, 2014; Gaillard, Ménézo, Giroux, Pabiou, & Le-Berre, 2014) were recently analysed.

For these reasons, a DSF-P numerical model was developed based on energy balance equations. The model has the ability to simulate the opaque or semi-transparent photovoltaics integrated on the exterior layer of the double skin façade as well as any shading devices inside the cavity including the shades that they provide to the building. (Figures 1 and 2). It is also capable to assess the active and passive effects of the generic DSF-P on the thermal and visual comfort and energy consumptions of the building in which the system is integrated.

The model also allows the user to perform a parametric analysis changing the design, and geometric parameters and the optical, thermal and flow properties of the DSF. These parameters can be seen on Table 1.

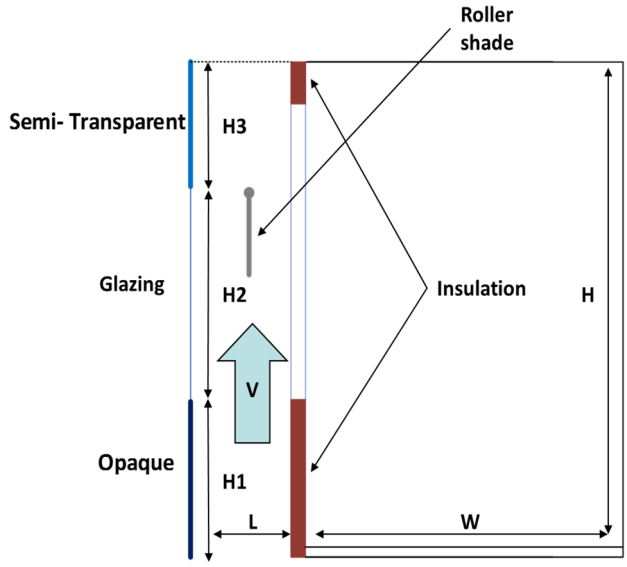

Figure 1. *Sketch of the double façade section (one story)*

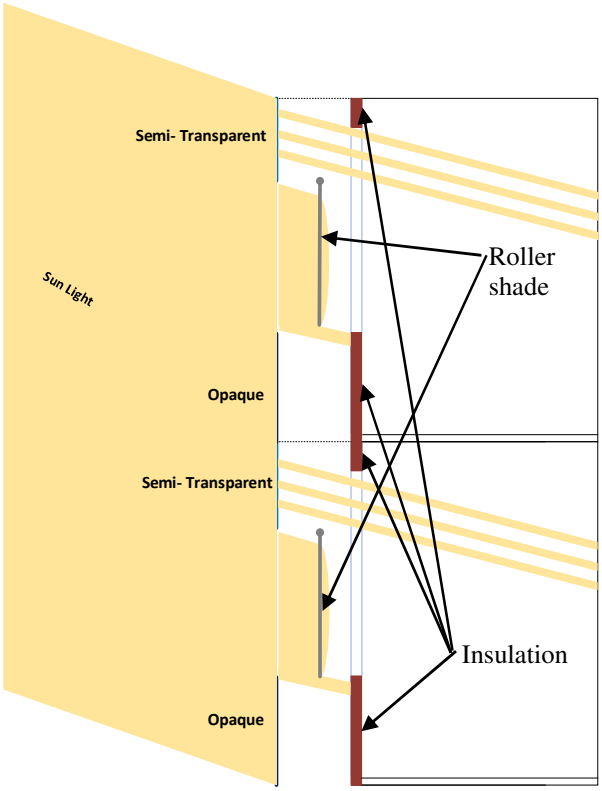

Figure 2. *Sketch of the double façade section (two stories), including the cavity and the roller shades. Light passes through the STPV to the room.*

Table 1

Design parameters	Number of floors Position of PV Position of roller blind Interior skin design
Geometric parameters	H1/H H2/H H3/H L/H W/H
Optical properties	STPV transmittance Roller shade transmittance Glazing transmittance
Thermal properties	PV efficiencies Roller emissivity SHCG Insulation of the room
Flow properties	Reynolds number Velocity

This model can be used for pre-feasibility studies, in the early stages of the design of buildings or of retrofit projects on existing buildings to be integrated with BIPV/T technology. The DSF-P takes full advantage of the cavity and especially of the buoyancy driven air flow inside the cavity, which serves the system in two ways: i) to absorb the heat from the integrated PV in order to decrease their temperature and hence, improve their electrical efficiency; ii) to utilize the preheated air as a source for natural or hybrid ventilation (heating or cooling) for the building. In addition, the air at the top of the cavity can be introduced directly into the building, if the outlet temperature of the air flowing inside the cavity is higher than the temperature of the building and it does not exceed the comfort levels of the occupants, or it can be introduced to the HVAC system as preheated air, in order to reduce the energy consumption. The modelled cavity also includes automated roller shades, which help the reduction of space cooling loads and control the daylight levels in the indoor space.

MODELLING

A mathematical model for the assessment of the energy performance of a multi-story Double Skin Façade (DSF) has been implemented in MatLab (Mathworks). The model also enables the prediction of the thermal effects of building integrated DSF systems on the heating and cooling consumption of the adjacent indoor air spaces. In this section, a brief description of the main thermal phenomena taken into account in the simulation model is presented.

The façade consists of a semi-transparent PV section, a so-called Vision section, and an Opaque section, as depicted in Figures 1 and 2. The separation wall between the cavity and the indoor air consists of two opaque elements (i.e. spandrels located at the top and bottom of the wall) and a glazing area at the middle of the wall, see Figure 1. Thus, the whole façade, and, similarly, the wall of a multi-story building are designed as multiple strips made of semi-transparent(ST), transparent, and opaque elements. Roller shades/blinds are located in the middle of the cavity in order to control the daylighting levels within the indoor space, Figure 2. Air flows on both sides of the two cavity channels coupled via such blinds.

The mathematical model of the DSF-P includes all of the heat transfer processes; utilizes an accurate nodal (finite volume) approach; and uses fast numerical solving processes. Therefore, a set of explicit equations, is obtained for each node of the adopted thermal Resistance Capacitance (*RC)* network, showing the conductive, radiative and convective heat transfers in the modelled DSF-P system. The *RC* thermal network schematic is given in Figure 3.

In order to capture the gradient of the air temperature along the cavity, each element of the multi-story DSF-P (i.e. the façade, the two air channels, and the wall) is subdivided, along the vertical direction, in *N* equal control volumes (i.e. *N* is suitably selected to enhance the accuracy of the simulation results), whose temperatures are calculated through the energy balance method. The multi-story building adjacent to the DSF-P is subdivided in *Z* different perimeter thermal zones as well.

Therefore, in each time step *t*, for each *z*-th perimeter zone and for each *n*-th section/node of the façade, the corresponding energy balance equation is calculated as:

$$\sum_{i=n-1}^{n+1}\frac{T_{f,i}-T_{f,n}}{R_{f,i}}+\frac{T_{db}-T_{f,n}}{R_{ext,n}}+\frac{T_{air,n}-T_{f,n}}{R_{ch,n}}+\ldots$$
$$\ldots+\dot{Q}_{f,n}+\dot{Q}_{rad,n}=0 \quad (1)$$

where T_f, T_{db} and T_{air} are the temperatures of the façade section, the ambient air and the air flowing within the channel; $R_{f,i}$ is the conductive resistance of each half sub-section of the façade (adjacent sections), $R_{ext,n}$ is the external convective resistance and $R_{ch,n}$ is the convective resistance calculated within the channels/cavity.

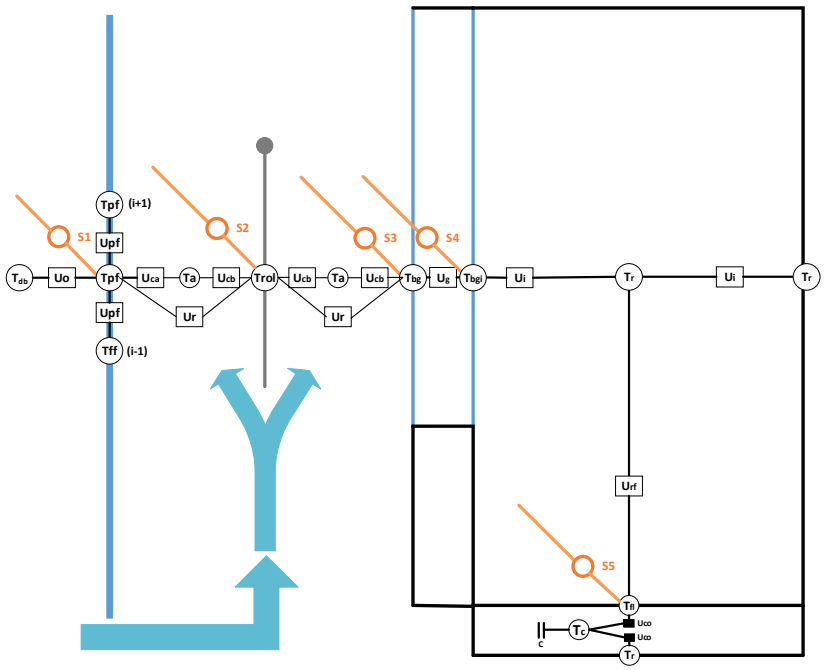

Figure 3 *Skematic of the thermal network model: nodal temperatures are given at each node connected with conductances U*

Two radiative gains are calculated while taking into account the effects due to the solar radiation on the thermal performance of the double façade: $\dot{Q}_{rad}$ is the net radiation exchange, due to the sum of the incoming radiation directly absorbed by the surface (considered as grey) and the radiative heat transfer between the exterior facade surface and the sky, whereas $\dot{Q}_f$ is the long-wave radiation exchange on the internal surfaces within the cavity. The radiative heat transfer problem within the channel is solved by assessing the view factors and the radiosities of all the sections constituting the cavity included between the façade and the facing surfaces, i.e. roller shades and/or wall. They are calculated as:

$$\dot{Q}_{rad,n} = \left[\alpha_{f,n} \cdot I_{f,n} + \varepsilon_n \cdot \sigma \cdot f \cdot (T_{sky}^4 - T_{f,n}^4)\right] \cdot A_n$$

$$\dot{Q}_{f,n} = A_n \cdot \sum_{i=1}^{N} \frac{\varepsilon_i}{1-\varepsilon_i} \cdot (E_{n,i} - J_i) \qquad (2)$$

where α_f and ε are the façade section absorptance and emissivity, I_f is the net incident solar radiation on the façade, f is the view factor between the façade section and the sky with temperature T_{sky} and A is the horizontal section surface area; E_n and J are the total emissive power and the radiosity of each surface, respectively.

The calculation of $\dot{Q}_{rad}$ is carried out by assuming the cavity sketched in Figure 1. Note that, the inlet and outlet sections of the cavity (i.e. the horizontal separation surfaces between the two adjacent cavities, each of them is adjacent to an indoor space) are assumed as black surfaces at a mean air temperature calculated through a backward procedure. In addition, the roller blind is also assumed as a grey and adiabatic surface and, consequently, as reradiating surface.

In the case of a section representing a semi-transparent PV layer, I_f is obtained by cutting the gross electrical power production, P_{el}, calculated as:

$$P_{el} = \eta_{PV} \cdot I_{f,n} \cdot A_n \qquad (3)$$

where η_{pv} is the PV efficiency, assumed linearly decreasing with the increasing operating temperature (Liao, 2005).

$$\eta_{PV} = \eta_{ce}[1 - \beta_{cl}(T_{cl} - 25^oC)] \qquad (4)$$

Regarding the interior skin of the double skin façade, two walls (nodes) who are separating the cavity from the indoor space are modeled: an exterior (facing the cavity) and an interior wall surface (facing the indoor space). Thus, N sections (along the vertical direction) for each of these surfaces and N resistive thermal nodes for each story, are taken into account. For such nodes, the boundary conditions are the air flowing within the cavity and the indoor air, respectively. In particular, similarly to equation (1), for each perimeter building zone and for each n-th section/node of the exterior and interior wall

surfaces, the corresponding energy balance equations are calculated as:

$$\frac{T_{air,n}-T_{wo,n}}{R_{ch,n}}+\frac{T_{wi,n}-T_{wo,n}}{R_{wl,n}}+\dot{Q}_{wo,n}+\dot{Q}_{rad,n}=0$$
$$\frac{T_{wo,n}-T_{wi,n}}{R_{wl,n}}+\frac{T_{in,k}-T_{wi,n}}{R_{int,n}}+\dot{Q}_{wi,n}=0 \quad (5)$$

where $T_{wo,n}$ and $T_{wi,n}$ are the temperatures of the exterior and interior wall sections, T_{in} is the indoor air temperature of the z-th building space. R_{wl} is the conductive resistance of the wall and $R_{int,n}$ is the internal convective resistance. $\dot{Q}_{wo,n}$ and $\dot{Q}_{wi,n}$ represent the effective solar radiation incident on the external and internal surfaces of the wall. These include the diffuse solar radiation and the net (transmitted and/or absorbed) beam solar radiation, suitably calculated by taking into account the cast shadows due to the façade surfaces and the roller blinds.

For the cavity, the buoyancy-driven air flow is assumed to be quasi steady and for each of the N control volumes in which each air channel is discretized, an energy balance is written. It must be noted that, due to the adopted formulation, the air temperature of the channels inside the double façade describes the radiation exchange, convection and mass transfer, including the identification of the heat transfer coefficients. As reported in previous studies, the temperature profile in a ventilated cavity is exponential (Charron & Athienitis, 2006). Thus, with the aim to avoid the use of an air temperature profile, the change of energy of each control volume is assumed equal to the energy transferred to the air by convection. This leads, after solving a first order differential equation of air temperature(Charron & Athienitis, 2006), to an expression that easily provides an exponential profile, such as:

$$T_{air,n}=\exp\left(-\frac{R_{ch,n}^{-1}+R_{ext,n}^{-1}}{\dot{m}_{air}\cdot c_{p,air}}\right)\cdot T_{air,n-1}+\ldots$$
$$\ldots+\left[1-\exp\left(\frac{R_{ch,n}^{-1}+R_{ext,n}^{-1}}{\dot{m}_{air}\cdot c_{p,air}}\right)\right]\times\ldots$$
$$\ldots\times\left(\frac{R_{ch,n}^{-1}\cdot T_{f,n}+R_{ext,n}^{-1}\cdot T_{wo,n}}{R_{ch,n}^{-1}+R_{ext,n}^{-1}}\right) \quad (6)$$

where $\dot{m}_{air}$ and $c_{p,air}$ are the mass flow rate and the specific heat capacity of the air flowing in each channel respectively. Note that, depending on the channel, different boundary conditions are taken into account and that, no air leakage is assumed in the DSF-P cavity. It is also assumed that uniform solar radiation is incident on clean exterior surfaces and PV modules are operating at their maximum power point condition.

The local Nusselt numbers Nu is used in order to represent the convective heat transfer coefficients along the channel height. Nusselt number correlations developed by Liao et al. (Liao et al., 2007) for the façade and internal side are used:

$$Nu_f=(0.011Re+62.856)e^{-0.475\frac{H}{L}}+(2.766x10^{-3})Re+5.58 \quad (7)$$

$$Nu_{int}=(0.109Re-124.34)e^{(-1.635x10^{-5}Re-0.593)\frac{H}{L}}+(4.098x10^{-3})Re+3.896 \quad (8)$$

Also by using the definitions of Nusselt and Reynolds numbers, the local convective heat transfer coefficients we been generated.

$$Nu=\frac{h_c L}{K_{air}} \quad (9)$$
$$Re=\frac{\rho V L}{\mu} \quad (10)$$

For each z-th indoor space adjacent to the DSF-P system, its indoor air is assumed as uniform and perfectly mixed. Therefore, a single lumped indoor air temperature node is taken into account. In order to assess the transient effects induced by the thermal mass the floor thermal mass is lumped in a single capacitive node, whereas the thermal effect of interior walls are disregarded (i.e. also assuming the same temperature in the core zones of the whole building). This entails that for each z-th zone, the differential equation describing the energy rate of change of each temperature node of the floor is calculated as:

$$T_{fl,z}^{t}=T_{fl,z}^{t-1}+\frac{\Delta t}{C_{fl,z}}\cdot\left(\dot{Q}_{fl,z}+\sum_{k=1}^{N}\frac{T_{wi,k}-T_{fl,z}^{t-1}}{\bar{R}_{rad,k}}+\frac{T_{in,z}-T_{fl,z}^{t-1}}{R_{fl,int}}\right) \quad (11)$$

being T_{fl} and C_{fl} are the temperature and the thermal capacitance of the floor capacitive node respectively; $\bar{R}_{rad}$ is the radiative thermal resistance between the internal wall surfaces and the floor, $R_{fl,int}$ is the combined convective and radiative thermal resistance between the indoor air and the floor; $\dot{Q}_{fl,z}$ is the solar heat source at the node.

Finally, the energy rate of change linked to the indoor air mass is:

$$T_{in,z}^{t} = T_{in,z}^{t-1} + \frac{\Delta t}{C_{in,z}} \cdot \left(\dot{Q}_{in,z} + \sum_{k=1}^{N} \frac{T_{wi,k} - T_{in,z}^{t-1}}{\bar{R}_{int,k}} + \frac{T_{fl,z} - T_{in,z}^{t-1}}{R_{fl,int}} \right) \quad (12)$$

where C_{in} is the thermal capacitance of the indoor air, $\bar{R}_{\text{int}}$ is the combined convective and radiative thermal resistance between the internal wall surfaces and the indoor, $\dot{Q}_{in,z}$ is the overall sensible heat gain networked to the indoor air node. Specifically, $\dot{Q}_{in,z}$ includes: i) the convective sensible internal gains due to occupants, lights and equipment, ii) the infiltration/ventilation thermal load (calculated as a function of the difference between the outdoor ambient air and the indoor one), iii) the sensible heat supplied to or removed from the building space to maintain the indoor air at the desired set point temperature. The latter is provided in case of the indoor air temperature, in free floating regime, is outside the heating or cooling regions at the end of a simulation time step. In this case it is assumed that the temperature change of the indoor air is linear. By following this approach, thermal power is added to or subtracted from $\dot{Q}_{in,z}$ with the aim to maintain the indoor air temperature at the desired set points.

Summarizing, homogeneous temperature in each control volume is assumed, each façade and building element construction material is assumed as uniform, whereas thermal properties (i.e. heat transfer coefficients, air density, PV efficiency, etc.) are calculated based on the control volume temperatures assessed by solving the whole set of algebraic and differential equations (1), (2), (5), (6), (11) and (12). The system is solved in each time step through a solver for systems of nonlinear equations included in MatLab (Mathworks).

SIMULATION

The simulations were carried out for a winter and a summer month (January and August respectively). The indoor office conditions were following a normal week-day schedule from 8.00 to 18:00 and the temperature was let to fluctuate between 21°C and 24°C. The simulations were carried out with one hour time step, compatible with a Typical Meteorological Year data file (TMY) of Montreal (Canada) was used as a source for the ambient weather conditions and the solar radiation. A reference office described by Reinhart et al. (Reinhart, Jakubiec, & Ibarra, 2013) was taken into account; with dimensions 2.8m height, 3.6m width and 8.2m length. The bottom spandrel is 1.0m high, the window is 1.5m high and the upper spandrel is 0.3m high giving a 55% window-to-wall ratio. The cavity width is set to be 0.5m, the roller is placed at the middle of the cavity (0.25m from both ends) and the transmittance of the STPV is set to be 30%.

Two different set-ups were examined, one being with one storey and the other with three storeys double skin façade. The different cases that were examined are presented on table 2:

Table 2

	Floors	Velocity	Roller
January	1	0.1m/s	down
			up
		0.2m/s	down
			up
August	1	0.1m/s	down
			up
		0.2m/s	down
			up
January	3	0.1m/s	down
			up
August	3	0.2m/s	down
			up

RESULTS

Temperature difference (ΔT) between the inlet and the outlet of the cavity is simulated for all different cases presented above. The maximum ΔT is presented on Table 3. It can be seen that the existence of a typical roller blind can contribute to higher temperature difference between the inlet and the outlet. This temperature difference is higher during the winter months when the ambient temperature is lower than the interior temperature. During the summer month (August) this temperature difference between the inlet and the outlet for the cases Roller up and Roller down decreases.

As the velocity of the air inside the cavity increases, the temperature difference between the inlet and the outlet of the cavity decreases. This difference is higher on January due to the fact that ambient temperature and solar altitude is lower. In this way, more solar radiation is absorbed by the roller blind resulting in an increase of the air temperature inside the cavity. This is also shown in Figures 4 and 5 for a typical winter (January 1st) and summer (August 1st) day for which the position of the roller blind for each floor can be seen. This temperature difference is very important because the cavity can work as a buffer zone during the cold months of the year and the preheated air can be introduced to the HVAC system.

For the three floors configuration, the contribution of each floor to the total DSF-P temperature is independent from the existence of a roller blind inside the cavity. Specifically, the first floor contributes 36.7%, the second 33.2% and the third 30.1%. About the same percentages are observed for both winter and summer seasons.

The temperature distirbution of the exterior skin is a very important parameter that must be simulated and predicted because on the exterior façade opaque and Semi-Transparent photovoltaics are integrated. As it can be seen from Figure 6 and 7 the temperature of the photovoltaics is among other parameters, a function of incident solar radiation and ambient temperature. When the velocity of the air cavity is set to be V=0.2m/s, the temperatures reached by the photovoltaics are up to 6°C lower than those obtained for V=0.1m/s, in both seasons. The other parameter that is of equal importance to the temperatures of the cavity and the photovoltaics integrated on the external skin, is the energy consumption and generation of the system.

Table 3 Air temperature difference between the inlet and the outlet of the DSF-P for all cases presented.

Temperature difference (°C)					
	Floors	v=0.1m/s		v=0.2m/s	
		Roller down	Roller up	Roller down	Roller up
January	1st	11.29	8.47	6.11	4.78
August	1st	7.93	6.84	4.48	4.23
January	1st			6.14	4.80
	2nd			5.57	4.35
	3rd			5.05	3.92
	DSF			16.76	13.07
August	1st			4.50	4.00
	2nd			4.04	3.58
	3rd			3.62	3.20
	DSF			12.16	10.78

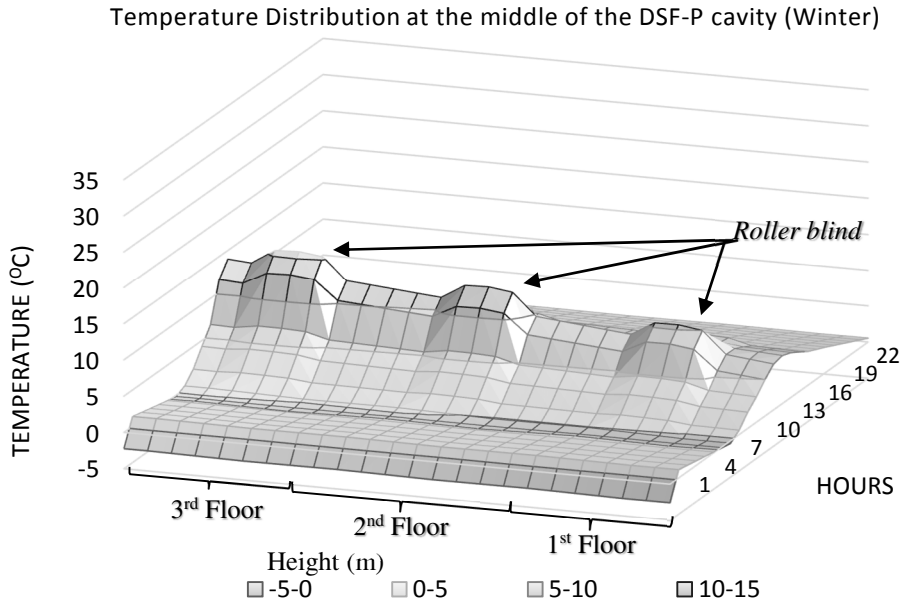

Figure 4. Effect of the increase of air temperature due to the existence of roller blind. For 3 floors DSF-P (8.4m height) in a period of a day under winter time conditions with shading device and V=0.2m/s.

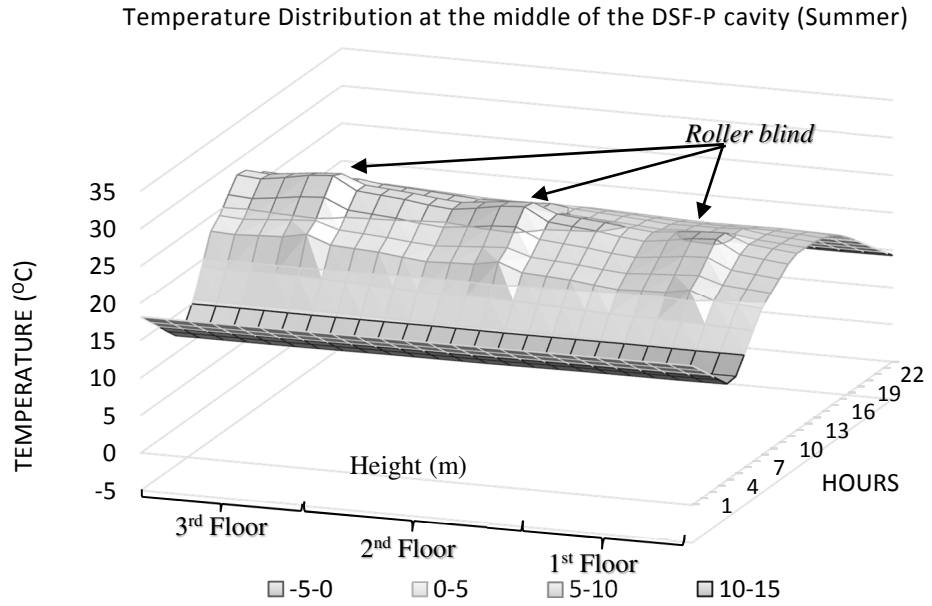

Figure 5. Effect of the increase of air temperature due to the existence of roller blind. For 3 floors DSF-P (8.4m height) in a period of a day under summer time conditions with shading device and V=0.2m/s.

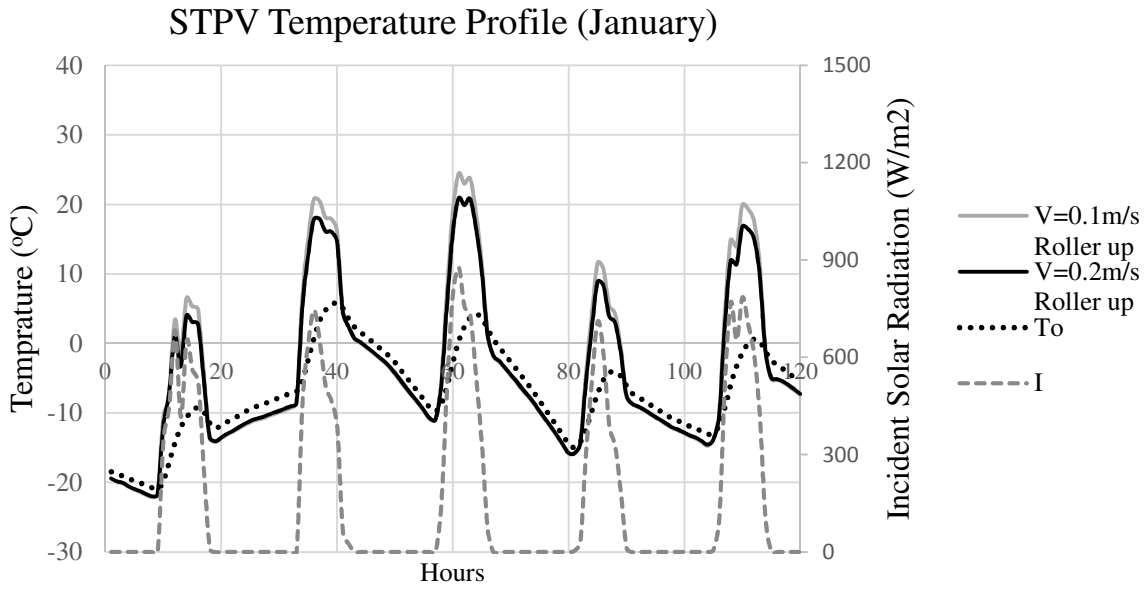

Figure 6. STPV temperature profile for a week of January for two different velocities inside the cavity, V=0.1m/s and V=0.2m/s.

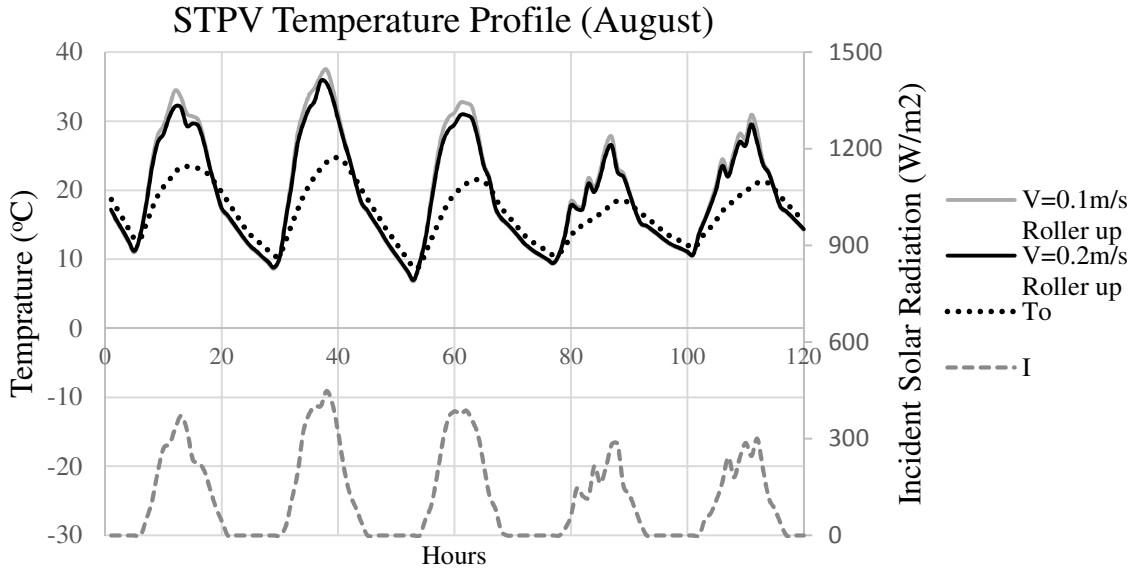

Figure 7. STPV temperature profile for a week of August for two different velocities inside the cavity, V=0.1m/s and V=0.2m/s.

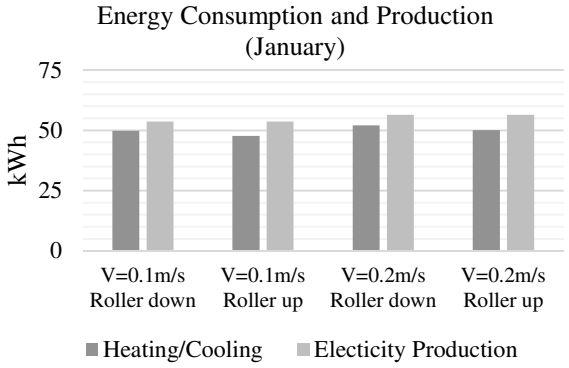

Figure 8. Comparison of energy consumption and generation during the heating season for velocities of 0.1m/s and 0.2m/s with and without shading.

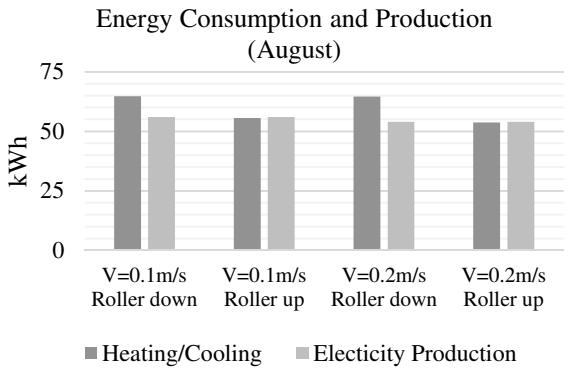

Figure 9. Comparison of energy consumption and generation during the cooling season for velocities of 0.1m/s and 0.2m/s with and without shading.

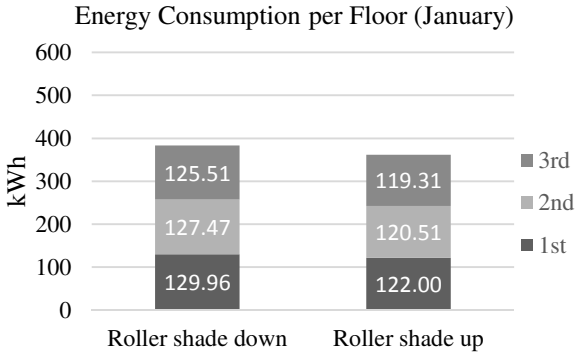

Figure 10. Comparison of energy consumption and generation during the cooling season for velocity of 0.2m/s with and without shading

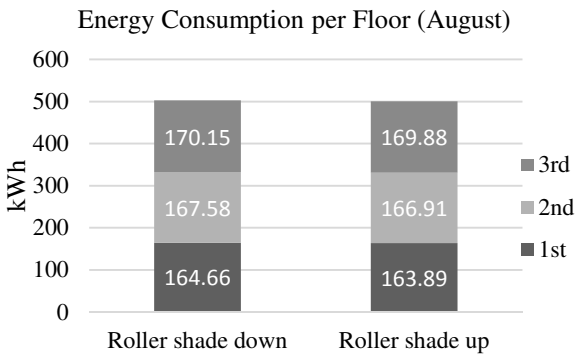

Figure 11. Comparison of energy consumption and generation during the cooling season for velocity of 0.2m/s with and without shading.

For a typical schedule (8.00 to 18:00) with set points of 21ºC and 24ºC the energy that is required to maintain the indoor air temperature between the levels of thermal comfort is presented on Figure 8 and Figure 9 for January and August respectively. On the same graphs, a comparison is held between the consumed energy and the energy in the form of electricity produced by the photovoltaic panels integrated on the DSF-P. A heat pump with a coefficient of performance equal to 2.5 is assumed to be the source of heating and cooling to the interior zone (ASHRAE, 2008). It is preferable for the heating season to keep the velocity inside the cavity lower and increase it during the cooling season. It can also be observed that for some cases, the total amount of energy used to heat or cool the room can be completely produced by the photovoltaics.

In the three story DSF-P configuration, less energy is required to maintain the temperature of the room between the set points for the higher floor during the heating season. The opposite behavior was observed during the cooling season where the higher floor needed more cooling loads in order to provide thermal comfort to the occupants. (Figure 10 and Figure 11). Other parameters, like lighting energy consumptions are not calculated since this paper is focusing on the behavior of the DSF-P. Although having in mind that the preheated air of the DSF-P can be introduced to HVAC system, then the energy generation from the PV of the system may be able to cover a large percentage of other electrical needs of the building.

CONCLUSION

In this paper a numerical model of a Double Skin Façade integrated with photovoltaics (DSF-P) is presented. The methodology that is followed and the equations that are used in order to simulate this multi-story DSF-P are also presented. With the aim to show the capability of the numerical model a set of simulations was carried out for January and August in Montreal, for different air velocities inside the cavity (V=0.1m/s and V=0.2m/s), different set-up for the roller blind (Roller up, Roller down) and different number of floors (one and three floors).

It is noted that the existence of a roller blind increases the temperature of the air inside the cavity and the temperature difference between the inlet and the outlet, but also decreases the efficiency of the integrated photovoltaics on the exterior skin of the DSF-P. The integrated photovoltaic panels can provide a large percentage of the energy used to heat or cool the adjacent zones and in some cases the amount needed for this purpose can be exceed. Also the simulations show that a DSF-P for a typical office (2.8m height, 3.6m width façade area) can generate approximately 0.20kWh/m^2/day of solar electricity.

Regarding the multi-story DSF-P, as the number of floor increases the energy needed to heat the room decreases (heating season) while the energy needed to cool the room (cooling season) increases.

Finally the model for the simulation and the assessment of the performance of a double skin façade integrated with photovoltaics was purposely developed to aid the design of buildings integrated with the proposed DSF-P system. The model is capable to carry out parametric and sensitivity analyses and it can be used for pre-feasibility studies at the construction phase of new buildings or for retrofit projects. The next step of the research is to add lighting and daylighting analysis to the model and also create control strategies to optimize the air flow rate inside the cavity and the position of the blinds.

ACKNOWLEDGEMENTS

The authors acknowledge the support of the Natural Sciences and Engineering Research Council of Canada (NSERC) through a NSERC/Hydro Quebec Industrial Chair. Also they wish to gratefully acknowledge Action TU1205 (Building Integration of Solar Thermal Systems, BISTS) of the European COST (Cooperation in Science and Technology), Transport and Urban Development (TUD), for the sponsorship and the precious scientific support.

NOMENCLATURE

A	heat exchange surface area (m^2)
BIPV/T	Building Integrated PV/Thermal
C	thermal capacitance (J/K)
cop	coefficient of performance (-)
c_p	specific heat capacity (kJ/kgK)
DSF-P	Double Skin Façade integrating Photovoltaics
E	total emissive power (W/m^2)
f	surface view factor (-)
H	total DSF height (m)
H_1	opaque PV height (m)
H_2	exterior glazing height (m)
H_3	ST-PV panel height (m)
h	Heat transfer coefficient W/(m^{2}K)
I	solar radiation flux (W/m^2)
J	radiosity (W/m^2)
K	thermal conductivity (W/mK)

L	room length (m)
$\dot{m}$	mass flow rate (kg/s)
N	node of the thermal network
$\dot{Q}$	thermal load (W)
PV	photovoltaic
R	thermal resistance (K/W)
Re	Reynold number (-)
ST	semi transparent
T	temperature (K)
t	time (s)
V	velocity (m/s)
W	room width (m)
Z	building space

Greeks letters

α	absorption factor (-)
β_{cl}	parameter that, for crystalline is (0.4%)
ε	emissivity (-)
η	photovoltaic efficiency (-)
η_{ce}	photovoltaic efficiency under standard conditions (15%)
μ	air viscosity (kg/ms)
σ	Stefan-Boltzmann constant ($5.67\ 10^{-8}$ W/m^{2}K^4)

Superscript/Subscripts

air	air of the channel
c	convection
ch	channel
cl	cell
db	dry bulb air
el	electricity
ext	external
f	façade
fl	floor
in	indoor air
int	internal
n	node of the thermal network
PV	photovoltaic
rad	radiation
sky	sky vault
wg	referred to water vapour gain
wi	interior wall section
wl	wall
wo	exterior wall section
z	building space

REFERENCES

ASHRAE. (2008). *ASHRAE HANDBOOK HVAC Systems and Equipment*.

Athienitis, A., & O'Brien, W. (2015). *Modeling, Design, and Optimization of Net-Zero Energy Buildings*. Retrieved from http://ca.wiley.com/WileyCDA/WileyTitle/productCd-3433030839,subjectCd-AR20.html

Barbosa, S., & Ip, K. (2014). Perspectives of double skin façades for naturally ventilated buildings: A review. *Renewable and Sustainable Energy Reviews*, *40*, 1019–1029. http://doi.org/10.1016/j.rser.2014.07.192

Charron, R., & Athienitis, A. K. (2006). Optimization of the performance of double-façades with integrated photovoltaic panels and motorized blinds. *Solar Energy*, *80*, 482–491. http://doi.org/10.1016/j.solener.2005.05.004

De Gracia, A., Castell, A., Navarro, L., Oró, E., & Cabeza, L. F. (2013). Numerical modelling of ventilated facades: A review. *Renewable and Sustainable Energy Reviews*, *22*, 539–549. http://doi.org/10.1016/j.rser.2013.02.029

Gaillard, L., Giroux-Julien, S., Ménézo, C., & Pabiou, H. (2014). Experimental evaluation of a naturally ventilated PV double-skin building envelope in real operating conditions. *Solar Energy*, *103*, 223–241. http://doi.org/10.1016/j.solener.2014.02.018

Gaillard, L., Ménézo, C., Giroux, S., Pabiou, H., & Le-Berre, R. (2014). Experimental Study of Thermal Response of PV Modules Integrated into Naturally-ventilated Double Skin Facades. *Energy Procedia*, *48*, 1254–1261. http://doi.org/10.1016/j.egypro.2014.02.142

Gratia, E., & De Herde, A. (2007a). Are energy consumptions decreased with the addition of a double-skin? *Energy and Buildings*, *39*, 605–619. http://doi.org/10.1016/j.enbuild.2006.10.002

Gratia, E., & De Herde, A. (2007b). The most efficient position of shading devices in a double-skin facade. *Energy and Buildings*, *39*, 364–373. http://doi.org/10.1016/j.enbuild.2006.09.001

Kala, S., Stathopoulos, T., & Suresh Kumar, K. (2008). Wind loads on rainscreen walls: Boundary-layer wind tunnel experiments. *Journal of Wind Engineering and Industrial Aerodynamics*, *96*(6-7), 1058–1073. http://doi.org/10.1016/j.jweia.2007.06.028

Liao, L. (2005). NUMERICAL AND EXPERIMENTAL INVESTIGATION OF BUILDING- INTEGRATED PHOTOVOLTAIC-THERMAL SYSTEMS, (September).

Liao, L., Athienitis, a. K., Candanedo, L., Park, K.-W., Poissant, Y., & Collins, M. (2007). Numerical and Experimental Study of Heat Transfer in a BIPV-Thermal System. *Journal of Solar Energy Engineering*, *129*(4), 423. http://doi.org/10.1115/1.2770750

Manz, H. (2004). Total solar energy transmittance of glass double facades with free convection. *Energy and Buildings*, *36*(2), 127–136. http://doi.org/10.1016/j.enbuild.2003.10.003

Matlab. (n.d.). Matworks. Retrieved from http://www.mathworks.com/

Oesterle, E. (2001). *Double-Skin Facades - Integrated Planning*. Munich Germany: Prestel.

Quesada, G., Rousse, D., Dutil, Y., Badache, M., & Hallé, S. (2012). A comprehensive review of solar facades. Transparent and translucent solar facades. *Renewable and Sustainable Energy Reviews*, *16*(5), 2643–2651. http://doi.org/10.1016/j.rser.2012.02.059

Reinhart, C. F., Jakubiec, J. A., & Ibarra, D. (2013). DEFINITION OF A REFERENCE OFFICE FOR STANDARDIZED EVALUATIONS OF DYNAMIC FAÇADE AND LIGHTING TECHNOLOGIES 1 Massachusetts Institute of Technology , Cambridge , MA 02139 , USA 2 Harvard University , Graduate School of Design , Cambridge , MA 02138 , USA. *13th Conference of International Building Performance Simulation Association*, 3645–3652.

Saelens, D., Roels, S., & Hens, H. (2008). Strategies to improve the energy performance of multiple-skin facades. *Building and Environment*, *43*, 638–650. http://doi.org/10.1016/j.buildenv.2006.06.024

Shameri, M. a., Alghoul, M. a., Sopian, K., Zain, M. F. M., & Elayeb, O. (2011). Perspectives of double skin façade systems in buildings and energy saving. *Renewable and Sustainable Energy Reviews*, *15*(3), 1468–1475. http://doi.org/10.1016/j.rser.2010.10.016